HAL
open science

# Computation and Visualization of Risk Assessment in Deep Brain Stimulation

Alexandre Bilger, Christian Duriez, Stéphane Cotin

▶ **To cite this version:**

Alexandre Bilger, Christian Duriez, Stéphane Cotin. Computation and Visualization of Risk Assessment in Deep Brain Stimulation. MMVR 21 - Medicine Meets Virtual Reality, Feb 2014, Manhattan Beach, California, United States. hal-00881694v1

**HAL Id: hal-00881694**

**https://inria.hal.science/hal-00881694v1**

Submitted on 8 Nov 2013 (v1), last revised 13 Mar 2014 (v2)

**HAL** is a multi-disciplinary open access archive for the deposit and dissemination of scientific research documents, whether they are published or not. The documents may come from teaching and research institutions in France or abroad, or from public or private research centers.

L'archive ouverte pluridisciplinaire **HAL**, est destinée au dépôt et à la diffusion de documents scientifiques de niveau recherche, publiés ou non, émanant des établissements d'enseignement et de recherche français ou étrangers, des laboratoires publics ou privés.

# Computation and Visualization of Risk Assessment in Deep Brain Stimulation Planning

Alexandre BILGER [a,1], Christian DURIEZ [a] and Stéphane COTIN [a]
[a] *Project-team Shacra - Inria Lille - Nord Europe Research Centre*

**Abstract.** Deep Brain Stimulation is a neurosurgical approach for the treatment of pathologies such as Parkinson's disease. The basic principle consists in placing a thin electrode in a deep part of the brain. To safely reach the target of interest, careful planning must be performed to ensure that no vital structure (e.g. blood vessel) will be damaged during the insertion of the electrode. Currently this planning phase is done without considering the brain shift, which occurs during the surgery once the skull is open, leading to increased risks of complications. In this paper, we propose a method to compute the motion of anatomical structures induced by the brain shift. This computation is based on a biomechanical model of the brain and the cerebro-spinal fluid. We then visualize in a intuitive way the risk of damaging vital structures with the electrode.

**Keywords.** Deep Brain Stimulation, risk planning, brain shift, simulation

## Introduction

Deep Brain Stimulation is a neurosurgical technique to treat medication-resistant motion disorders symptoms, such as Parkinson's disease and essential tremor, or affective symptoms such as major depression. It consists in electrically stimulating a specific structure in the deep brain tissue. The surgical procedure involves the implantation of one (unilateral) or two (bilateral) stimulating electrodes. The electrodes are then left in the brain, attached to the skull and linked to a neurostimulator, which sends the electrical impulses.

Before the operation, the surgeon needs to determine the target coordinates in the patient frame, as well as a trajectory to reach the target. The path is linear and has to follow some surgical constraints, such as avoiding vital structures (e.g. blood vessels and ventricles), since the dissection of these structures could cause severe surgical complications. Currently the planning phase relies entirely on pre-operative data (which are a combination of the patient pre-operative image and an atlas containing detailed anatomical information). However, intra-operative brain deformation, called brain shift, can alter the pre-operative planning, since vital structures may have moved in the path of the electrode. This risk is limited by selecting a trajectory not too close from vital structures, in case of brain shift. In practice, this is done by defining a circle (typically with a radius

[1] Corresponding Author: E-mail: alexandre.bilger@inria.fr.

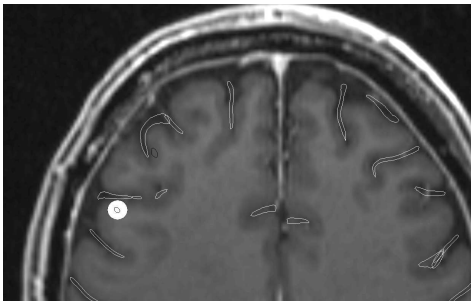

**Figure 1.** Considering a 4mm safety margin (in white) around an electrode path in classic pre-operative planning, the close blood vessel risks to be damaged if it shifts toward the trajectory

of 5mm), centered along the planned trajectory. This safety margin also includes errors due to the fusion and registration methods used during the planning (see Fig. 1). This geometric approach does not correctly describe the complexity of tissue motion during the brain shift. In particular, the brain shift induces an anisotropic tissue motion, while describing the safety margin as a circle assumes an constant isotropic motion.

We propose an advanced, more accurate method which better accounts for the complexity of the brain shift when selecting a safe trajectory. It consists in visualizing a volume around a candidate trajectory, which includes information about the brain tissue motion, based on a biomechanical simulation of brain shift. Our intention is to improve the current planning procedure without changing the surgeon's habit. In our method, the surgeon will check if a vessel is inside a complex closed shape, rather than a simple circle. In the physics-based approach, it means the vessel will shift towards the trajectory, and can potentially be damaged during the electrode insertion.

To achieve this goal, we propose a framework that reproduces the intra-operative brain tissue deformation. It includes a physics-based model of the brain, mechanicals interactions between the brain and the skull, and the influence of the cerebro-spinal fluid (CSF). The framework is based on our previous work [2]. Similar works modeled the brain shift phenomena, but a few included the interaction with the CSF [3]. Other works such as [9] use external virtual forces to register intra-operative images. A precise prediction of brain shift is difficult as some parameters (e.g. CSF loss volume) are unknown at the time of the planning. That is why most of the papers present methods to model the brain shift with intra-operative data. Our method does not predict the exact brain shift, but prevents risky electrode trajectories with a risk volume notion. The following section shows how we model the brain shift, then we present an intuitive way to visualize a risk to intersect vital structure with the electrode.

## 1. Methods & Materials

### *1.1. Numerical Simulation of Brain Shift*

Our simulation relies on a physics-based model of the brain tissue deformation, the contact response with the skull and the falx cerebri, and the interaction with the CSF. The brain deformation is computed using a non-linear geometric finite element method model, with a linear constitutive law [5]. The model is adapted for large displacements

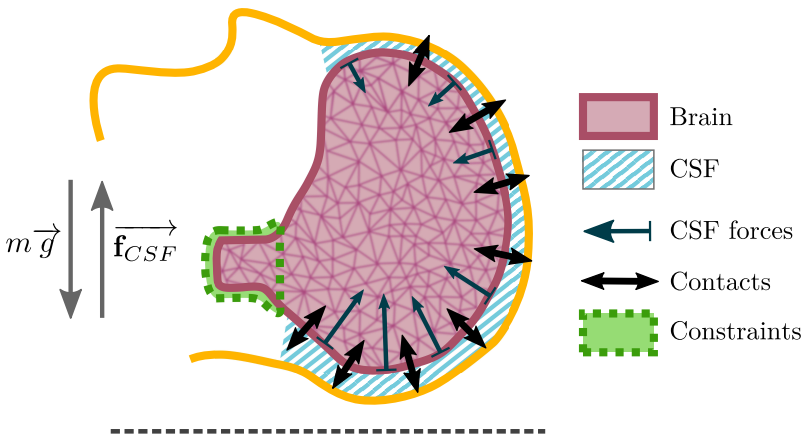


**Figure 2.** Schematic representation of the brain model and the set of constraints describing its interactions with the environment. In this pre-operative configuration, the patient is in the supine position (see the gravity vector direction $\overrightarrow{g}$). The cerebro-spinal fluid surrounds the brain tissue and acts on it with pressure forces. The resultant force balances the weight (see the $\overrightarrow{\mathbf{f}_{CSF}}$ compared to the weight force $m\overrightarrow{g}$). The brain is under a null displacement constraint near the brainstem area. The illustration also shows the potential contacts between the brain and the skull.

and small deformations, and is fast to compute for a clinical use. Although this model is linear, compared to more complex laws [8], it is a good trade-off between precision and computation time. Both brain hemispheres are meshed with approximatively 2500 linear tetrahedral elements. The Young's modulus is set to 6000 *Pa* and Poissons ratio to 0.45. The simulation computes the contacts between the brain, the inner part of the skull and the falx cerebri. They are detected using Layered Depth Images [6] and controlled using constraints solved with Lagrange Multipliers [1]. A null displacement constraint is set on both hemispheres near the area of the brainsterm. Figure 2 illustrates the different constraints and interactions in our simulation.

The main cause of brain shift is a CSF loss, happening after the skull opening. In rest position, the fluid forces and the gravity force are balanced. But after the skull opening, fluid leaks and fluid forces decrease. As the brain is more influenced by its weight than by fluid forces, this results in a brain shift. In order to account for this important phenomenon, we include a model of the CSF in our framework. Despite the development of computational fluid dynamics adapted for the CSF (e.g. [7]), a force model is sufficient in a brain shift simulation context, that is why we use the following model of fluid forces [3] that apply on the brain surface:

$$\mathbf{f}_{CSF} = \iint_S \rho\, g\, h(P)\, \mathrm{d}\mathbf{S}$$

where $\rho$ is the density of CSF (1000 $kg/m^3$), $g$ is the norm of the gravity and $h$ is the distance between a point $P$ on the mesh and the fluid surface. To compute the impact of the CSF onto the finite element model of the brain, the force $\mathbf{f}_{CSF}$ is applied onto every immersed triangle $S$ of the brain surface mesh.

To compute the brain deformation in the presence of CSF and under the boundary conditions described previously, we solve the following static differential system of non-linear equations:

$$K(u)\,u = \mathbf{f}_{CSF} + \mathbf{g} + \mathbf{H}^T\lambda$$

where $K$ is the stiffness matrix that depends on the displacement $u$ between initial configuration and deformed configuration, $g$ is the acceleration due to gravity and $\mathbf{H}^T\lambda$ gathers constraints response resulting from unilateral contacts and Dirichlet boundary conditions.

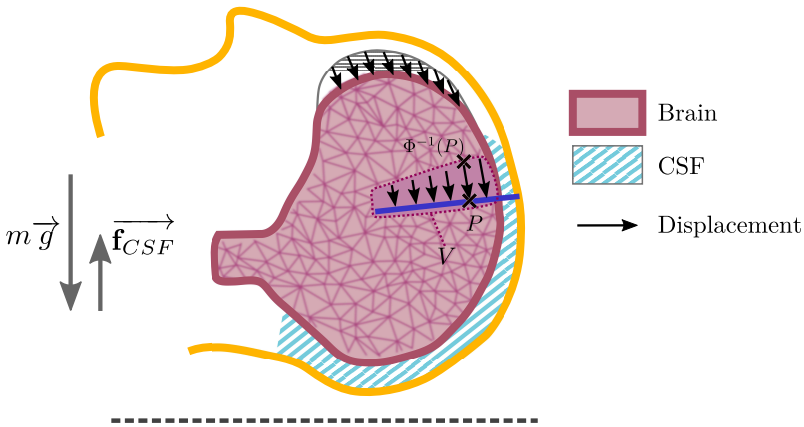


**Figure 3.** Schematic representation of the brain shift phenomenon. Due to the CSF loss (compared to figure 2), the fluid forces do not counterbalance the gravity force (see the two vectors). This leads to a brain shift, and the structures located in the vicinity of the electrode trajectory may move towards the electrode, increasing the risk of damaging vital structures. The risk volume $V$ (section 1.2) is represented with the associated displacement field $\Phi$.

### *1.2. Risk visualization*

To assess the risk of perforating with vital structures during the insertion of the electrode, we propose to visualize the result of the brain deformation in a natural way. To this end, we introduce the notion of risk volume associated to an electrode path. This risk volume is inspired from current clinical practice. In classic pre-operative planning, a constant safety margin is defined around the planned trajectory (see Fig. 1). In practice, this safety margin defines a cylinder, centered around the electrode axis, with a radius of a few millimeters. This safety margin encompasses various uncertainties in the location of the target and other anatomical structures, due to image registration errors, as well as a potential brain shift. In this paper, we propose to compute more precisely the safety margin as a risk volume that depends on the brain tissue motion, rather than a simple geometry. This risk volume is a combination of an omnidirectional geometric safety margin representing the unpredictable image processing errors, and a physics-based directional safety margin accounting for brain deformation. The computation of the physics-based safety margin is based on our biomechanical simulation, therefore the risk volume handles: the trajectory angle in the patient frame, the depth in the brain tissue and the orientation of the patient's head compared to gravity direction.

As mentioned previously, our approach consists in visualizing the risk that a structure might shift on the trajectory at the time of the surgery. We use this assumption in our algorithm to compute the risk volume associated to a given trajectory: let $V$ be the risk volume. Now, let $T$ be the trajectory, i.e. the segment defined between the target and a point on the surface of the skull, and $P \in T$ the points defining the trajectory segment. We also define the displacement field $\Phi$ joining the undeformed configuration and the deformed configuration due to the brain shift. We now compute the points $P_0$ such as $\forall P \in T,\ \Phi(P_0) = P$, hence $P_0 = \Phi^{-1}(P)$. $V$, $T$, and an example of $P$ and $P_0$ are depicted in figures 3 and 4. To compute $P_0$, we use the interpolation functions $N_i^e$ of an element $e$, with $i \in [1,4]$ in case of linear tetrahedrons. Let us find the element $e$ such as $P \in e$, then using the shape function of the tetrahedral finite element model, we have $P_0 = \sum_{i=1}^{4} N_i^e(P)\, x_0^{e,i}$. Here $\{x_0^{e,i} | i \in [1,4]\}$ is the coordinates of the nodes in the element $e$ of the underformed brain. Finally, we obtain a volume risk $V = \{x \in \mathbb{R}^3 \mid \|x - x_p\| \leq r,\ \forall x_p \in [P, \Phi^{-1}(P)],\ \forall P \in T\}$, with $r$ an error parameter handling the errors due to the model and the image processing uncertainties. The following section presents our results.

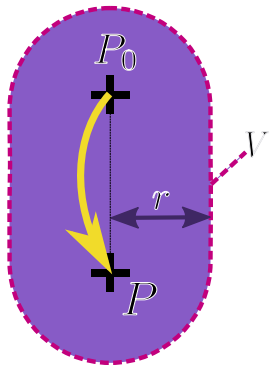


**Figure 4.:** 2d illustration showing an example of a point $P$ on the trajectory, and its associated point $P_0 = \Phi^{-1}(P)$. $V$ is represented depending on $r$.

## 2. Results

In this section, we present the results of our method, applied on a high-fidelity anatomical 3D model of the brain. It includes brain tissues, skull, falx cerebri, ventricles, vessels and the target (subthalamic nucleus). In our tests, we assume the target coordinates are already defined. First results are shown in figures 5 and 6. In these tests, we compare the physics-based risk volume and the geometry-based risk volume. We notice the physics-based volume is larger, making the trajectory selection more restrictive (see Fig. 8 com-

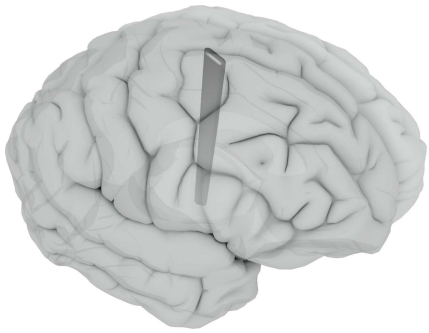

**Figure 5.** 3D representation of the physics-based risk volume in the cerebral environment. The risk volume is computed for a trajectory of an electrode implanted in the right hemisphere, represented in transparent.

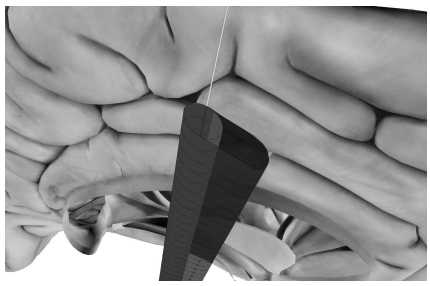

**Figure 6.** Close-up in the 3D representation of the physics-based risk volume (darker shape), compared to the geometry-based safety margin (cylinder).

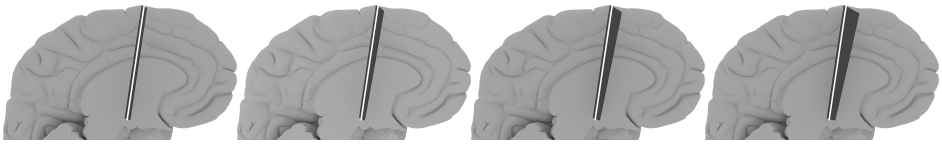

**Figure 7.** Variation of the risk volume depending on the CSF loss volume: from 10% lost (left), to 40% (right). The same trajectory for the four simulations is drawn in white.

pared to Fig. 1). Moreover, we observe the restriction acts mainly in the direction of the brain shift. Finally, we notice that the dimension of the volume in the direction of the brain shift varies depending on the depth in the brain tissues (see Fig. 5 and 6). This is due to the fact that the tissues on the surface have a larger motion than the deep tissues.

Our method applies in the pre-operative planning step, at which point we do not know the CSF volume that will be lost during the surgery. Besides, there is no precise model to anticipate it. The CSF loss depends on many parameters: orientation of the patient's head, burr hole location, anatomy, pathology etc. For this reason, we ask the surgeon to select an amount of CSF loss, expressed in percentage from 0% (no CSF loss) to 100% (all the CSF of the intracranial cavity has leaked out). Different CSF losses have been tested, and are depicted in figure 7. It appears that the more the brain shift, the larger the risk volume, as expected. Although, the amount of CSF loss is difficult to evaluate, we have determined from the literature [4] that a realistic spectrum of percentage is between 0%-40% (knowing that 40% is a huge value that happens in some rare cases). Depending on the pathology and its known relationship with the amount of brain shift (e.g. atrophy of the brain), the surgeon can adjust the value of CSF loss to better estimate the intra-operative scenario. It is also known that the surgical technique has an impact on the CSF loss (e.g. dura mater opening). There is obviously a duality between the brain shift and the CSF loss volume, therefore we can also define a brain shift amplitude based on a displacement, rather than a CSF loss.

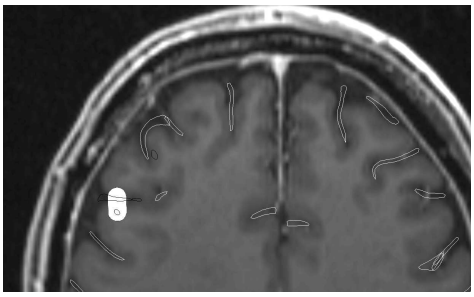

**Figure 8.** With our visualization of brain shift risk, vessels which can shift toward a trajectory are detected.

## 3. Conclusion

In conclusion, we propose a method to intuitively visualize a risk assessment in DBS planning. The computation is based on a physics-based brain shift simulation, handling the trajectory angle, the depth in the brain tissue, and the patient's head orientation.

Morevoer, with a more advanced biomechanical model of the brain, we will be able to include more variations in the risk volume: heterogeneity and anisotropy of the brain tissue, interactions with the vascular network.

As there is a duality between brain shift and CSF loss, our next step is to use intra-operative images to retrieve the brain state with the fitting parameters in our brain shift simulation.

## Acknowledgments

The authors would like to thank the French Research Agency (ANR) for funding this study through the Acoustic project (ANR 2010 BLAN 020901). The authors would also like to thank the Acoustic members for their participation in the useful discussions about this work: Éric Bardinet, Tiziano D'Albis, Caroline Essert, Sara Fernandez Vidal, Noura Hamze, Pierre Jannin, Gregory Laheurte and Jérôme Yelnik.

## References

[1] Jérémie Allard, François Faure, Hadrien Courtecuisse, Florent Falipou, Christian Duriez, and Paul G Kry. Volume contact constraints at arbitrary resolution. *Transactions on Graphics (Proceedings of SIGGRAPH 2010)*, 29(4):1–10, 2010.

[2] Alexandre Bilger, Jérémie Dequidt, Christian Duriez, and Stéphane Cotin. Biomechanical simulation of electrode migration for deep brain stimulation. *Proc. Medical Image Computing and Computer-Assisted Intervention (2011)*, 14(1):339–346, January 2011.

[3] Olivier Clatz, Hervé Delingette, Eric Bardinet, Didier Dormont, and Nicholas Ayache. Patient-specific biomechanical model of the brain: application to Parkinson's disease procedure. *Proceedings of the 2003 international conference on Surgery simulation and soft tissue modeling*, pages 321–331, 2003.

[4] W Jeffrey Elias, Kai-Ming Fu, and Robert C Frysinger. Cortical and subcortical brain shift during stereotactic procedures. *Journal of neurosurgery*, 107(5):983–8, November 2007.

[5] C Felippa and B Haugen. A unified formulation of small-strain corotational finite elements: I. Theory. *Computer Methods in Applied Mechanics and Engineering*, 194(21-24):2285–2335, June 2005.

[6] Bruno Heidelberger and M Teschner. Detection of collisions and self-collisions using image-space techniques. *Journal of WSCG*, 2004.

[7] Vartan Kurtcuoglu. Computational fluid dynamics for the assessment of cerebrospinal fluid flow and its coupling with cerebral blood flow. In *Biomechanics of the Brain*, pages 169–188. Springer, 2011.

[8] Adam Wittek, Grand Joldes, and Karol Miller. Algorithms for computational biomechanics of the brain. In *Biomechanics of the Brain*, pages 189–219. Springer, 2011.

[9] Adam Wittek, Ron Kikinis, Simon K Warfield, and Karol Miller. Brain shift computation using a fully nonlinear biomechanical model. *Proc. Medical Image Computing and Computer-Assisted Intervention (2005)*, 8(2):583–590, January 2005.